PHYSICAL REVIEW B VOLUME 2, NUMBER 6 15 SEPTEMBER 1970

# Dielectric Enhancement and Mobility of $\alpha$-Sn

L. Liu*
*Department of Physics, Northwestern University, Evanston, Illinois 60201*
*and Gruppo Nazionale di Struttura della Materia, Sezione di Pisa, Italy*

and

E. Tosatti
*Scuola Normale Superiore, Pisa, Italy*
*and Gruppo Nazionale di Struttura della Materia, Sezione di Pisa, Italy*
(Received 2 January 1970)

The static dielectric function $\epsilon(q)$ for degenerate $n$-type $\alpha$-Sn has been calculated for small $q$. Owing to the fact that the degeneracy of the contact point between the conduction and valence bands is symmetry induced, the dielectric constant has a strong dependence on impurity concentration and is greatly enhanced in value for low-doping concentrations. This dielectric enhancement gives an excellent quantitative account of the observed high-mobility values at low temperature (4.2 °K).

## I. INTRODUCTION

Among semiconductors, $\alpha$-Sn has very high electron mobility. This is usually attributed to the small effective mass of the electrons in the central minimum of the conduction band. It has been noted, however, that the smallness of the effective mass alone can not quantitatively account for the measured high-mobility value at low temperature (4.2 °K) for the lightly doped samples. One is led to look into the strength of the scattering mechanism itself for other possible explanations of the observed anomolously large mobility values. At the low-temperature region, the impurity ions are the dominant sources to scatter electrons off.

As for the question of the screening of the impurity potential, several people[1,2] have studied the static dielectric constant $\epsilon(q)$ of a pure sample of $\alpha$-Sn and found that $\epsilon(q)$ goes to infinity like $\lambda/q$, as $q \to 0$. This infinity comes from the interband coupling between states near the degenerate band edge where the conduction and valence bands make contact.[3] For an actual sample of $\alpha$-Sn, however, the presence of impurity carriers is sufficient to remove this infinity. On the other hand, the metallic-type screening from intraband coupling now comes into play and contributes a Fermi-Thomas term to the dielectric constant. Lavine and Ewald[4] have shown that even with the Fermi-Thomas screening, not only the mobility value itself but also its rate of increase as a function of impurity concentration $n$ in the range $n \sim 10^{17}$–$10^{14}$ is not accounted for. They had to fit the mobility data by assuming in addition a concentrational-dependent dielectric constant.

The present paper deals with the concentrational-dependent static dielectric constant for a $n$-type degenerate sample of $\alpha$-Sn. We show that it has the same origin as the one giving rise to an infinite dielectric constant for the pure sample, which is the interband transition near the degenerate band edge. We calculate $\epsilon(q)$ for $0 \le q \le 3k_F$ where $k_F$ is the Fermi momentum of the degenerate donor electrons. With the complete $\epsilon(q)$ we evaluate the electron mobility due to impurity scattering.

We present the dielectric-constant calculation in Sec. II and the mobility calculation in Sec. III. Finally, in Sec. IV, we discuss the situation with respect to other zero-gap materials.

## II. STATIC DIELECTRIC CONSTANT

In discussing the dielectric constant for a degenerate $n$-type sample of $\alpha$-Sn, we divide it up into three parts:

$$\epsilon(q) = \epsilon_0 + 4\pi\,\alpha^{\text{inter}}(q) + 4\pi\,\alpha^{\text{intra}}(q)\ . \tag{2.1}$$

The interband coupling between the valence-band and conduction-band states close to the edge ($k < q$) gives rise to a polarizability which we denote by $\alpha^{\text{inter}}$, and the intraband excitation of the impurity carriers gives rise to $\alpha^{\text{intra}}$. Transitions between valence and conduction states at $k > q$ as well as transitions among all other bands or between all other bands and the conduction- or valence-band contribute a $q$-independent part $\epsilon_0$. Among the three parts, $\epsilon_0$ is known experimentally[5] to be 24 and $\alpha^{\text{intra}}$ should be appropriately given by the Fermi-Thomas expression $4\pi\alpha^{\text{intra}} = k_{\text{FT}}^2/q^2$ for small $q$. It is the part $\alpha^{\text{inter}}$ which we calculate in detail. It turns out that although $\alpha^{\text{inter}}$ remains finite in a doped sample, it has a strong dependence on the impurity concentration $n$ and can reach a high

value when $n$ becomes small.

In a two-band approximation, the random-phase-approximation (RPA) interband dielectric constant is given[6] by

$$\epsilon^{\text{inter}}(q) = 1 - \frac{8\pi e^2}{q^2} \sum_k \frac{|\langle \vec{k}, c \,|\, e^{-i\vec{q}\cdot\vec{r}} \,|\, \vec{k}+\vec{q}, v\rangle|^2}{E_{\vec{k}+\vec{q},v} - E_{\vec{k},c}} \times (N_{\vec{k}+\vec{q},v} - N_{\vec{k},c}) , \qquad (2.2)$$

where the Bloch state $|\vec{k}, n\rangle$ has energy $E_{\vec{k},n}$ and occupation number $N_{\vec{k},n}$ with $n = c$ or $v$ specifying conduction or valence band, respectively. The coupling matrix element in (2.2) is just the overlap integral between the periodic part of the conduction-state and valence-state Bloch functions. This has been evaluated in the $\vec{k}\cdot\vec{p}$ approximation[1,2] to be

$$|M|^2 \equiv |\langle \vec{k}, c \,|\, e^{-i\vec{q}\cdot\vec{r}} \,|\, \vec{k}+\vec{q}, v\rangle|^2 = \frac{3}{4}\, \frac{(\vec{k}\times\vec{q})^2}{k^2(\vec{k}+\vec{q})^2} . \qquad (2.3)$$

Under the same approximation, both energy bands are warped. For simplicity, we neglect the warping and assume spherical bands $E_{k,c} = \hbar^2k^2/2m_e^*$ and $E_{k,v} = -\hbar^2k^2/2m_h^*$, with energy measured from the band edge.

Because of the use of the $\vec{k}\cdot\vec{p}$ approximation and of the two-band model, $\epsilon_0$ is not correctly evaluated. As mentioned before we use the experimental value instead. We compute $4\pi\alpha^{\text{inter}}(q) = \epsilon^{\text{inter}}(q) - \text{const}$ from (2.2). The Pauli principle requires the interband coupling to be present only when the final state lies outside the sphere of radius $k_F$ occupied by the degenerate donor electrons. This part of the calculation would have been exact in the small-$q$ limit if not for the approximation of neglecting $m_e^*/m_h^*$ as compared with 1. This is equivalent to using $m_e^*$ for the reduced mass of the electron-hole pair. For α-Sn,[7,8] $m_e^* = 0.024m$ and $m_h^* = 0.26m$, this approximation only introduces an error not exceeding 10%. The actual calculation is presented in Appendix A and the final result is given below:

$$4\pi\alpha^{\text{inter}} = 6e^2 m_e^* f(q)/\pi\hbar^2 k_F + O(q), \qquad q \text{ and } k_F \ll K \qquad (2.4)$$

where $O(q)$ is some function whose value is negligibly small for small $q$ and hence of no concern to us and $K$ is the Brillouin-zone radius. The function $f(q)$ is independent of any parameter of the sample and is given in (A7). A plot of it is given in Fig. 1.

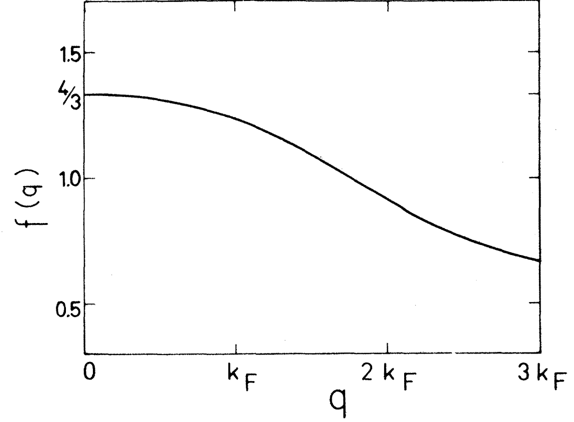


FIG. 1. The function $f(q)$.

TABLE I. Values of interband dielectric constant.

| $n(\text{cm}^{-3})$ | $10^{14}$ | $10^{15}$ | $10^{16}$ | $10^{17}$ | $10^{18}$ |
|---|---|---|---|---|---|
| $\epsilon_I(q=0)$ | 105 | 62 | 42 | 32 | 28 |

We also present in Table I the complete interband dielectric constant $\epsilon_I \equiv \epsilon_0 + 4\pi\alpha^{\text{inter}}$ for several impurity concentration values. As seen from the table, the dielectric constant is greatly enhanced in value for low impurity concentrations. This great enhancement of dielectric constant leads to the observed enhancement of low-temperature electron mobility. This we discuss in detail in Sec. III.

## III. ELECTRON MOBILITY

The dominant scattering mechanism contributing to the low-temperature mobility is the impurity scattering. We, therefore, start this section with a discussion on the screening of the bare impurity potential. We may use the explicit form of $k_{\text{FT}}^2/q^2$ for $4\pi\alpha^{\text{intra}}$ and rewrite the total dielectric constant in (2.1) in the following form:

$$\epsilon(q) = \epsilon_I(q)[1 + k_{\text{FT}}^{\text{eff}}(q)^2/q^2] , \qquad (3.1)$$

where $k_{\text{FT}}^{\text{eff}}(q) = k_{\text{FT}}/[\epsilon_I(q)]^{1/2}$ is the effective Fermi-Thomas screening parameter. Corresponding to the two multiplicative factors in (3.1), there are two effects produced by an enhanced $\epsilon_I$. One effect is a reduction in the strength of the impurity potential and the other is an increase in the effective Fermi-Thomas screening length. They produce opposite results in the impurity scattering cross section. However, the first effect dominates the second and the observed sharp increase of the low-temperature mobility with decreasing concentration can then be explained.

To discuss the question quantitatively, we note that the mobility $\mu$ for a degenerate sample[9] is giv-

en by

$$\mu = |e| (\hbar k_F n A)^{-1} \quad , \tag{3.2}$$

where $A$ is the total cross section for momentum transfer and is related to the differential cross section $\sigma(\theta)$ by

$$A = \int \sigma(\theta)(1 - \cos\theta)\, d\Omega \ . \tag{3.3}$$

We assume the bare impurity potential to be Coulomb and screened by $\epsilon(q)$ in (3.1). The form factor is then

$$V_s(q) = -4\pi e^2/\epsilon(q) q^2 \ . \tag{3.4}$$

Owing to the $q$ dependence of $\epsilon_I$, the screened impurity potential $V_s(r)$ is no longer of the Yukawa form $\exp[-k_{FT}^{eff}(0)r]/\epsilon_I(0)r$, which is appropriate for charged impurities in ordinary semiconductors. To simplify the form of the potential for the mobility evaluation, we use the following expansion for $f(q)$:

$$f(q) = \tfrac{4}{3}[1 - a(q/k_F)^2] \ . \tag{3.5}$$

This expansion is clearly suggested by Fig. 1, and the value for the constant $a$ is about $\frac{1}{12}$.

We calculate the differential scattering cross section for the screened impurity potential $V_s$ using the Born approximation. For the case under consideration, the Born approximation is valid because of the weakness of the potential. The question of validity is discussed in Appendix B. The cross section is then given by the well-known relationship

$$\sigma(\theta) = |(m_e^*/2\pi\hbar^2)\, V_s(q)|^2 \ , \tag{3.6}$$

where the momentum transfer $q = 2k_F \sin\frac{1}{2}\theta$. The quantity $A$ in (3.3) is then calculated to first order in $a$ in Appendix C. From (3.2), (C4), (C5), and (C9) we obtain the mobility

$$\mu = (3\pi |e| / 2\hbar)[\epsilon_I(0) \mathfrak{a}_\infty^*]^2 \{g(b) + 8a[1 - \epsilon_0/\epsilon_I(0)]\}^{-1}, \tag{3.7}$$

where $g(b)$ represents the zero-order term arising from Yukawa potential and is given in (C6) explicitly. The quantity $\mathfrak{a}_\infty^* = \hbar^2/m_e^* e^2$ is the effective Bohr radius for the electron.

Using the values of $\epsilon_I(0)$ from Table I and $m_e^* = 0.024m$ and $a = \frac{1}{12}$, the mobility is calculated as a function of $n$ and shown in Fig. 2 for $n = 10^{14}$–$5 \times 10^{17}$ cm$^{-3}$. The experimental mobility values[4,7,10] at 4.2 °K where impurity ions are expected to provide the dominant scattering mechanism are also shown. The range of the impurity concentration is chosen based on the following consideration. Since $\alpha$-Sn has a zero energy gap, the impurity atoms are ionized at all temperatures.[11] Then at

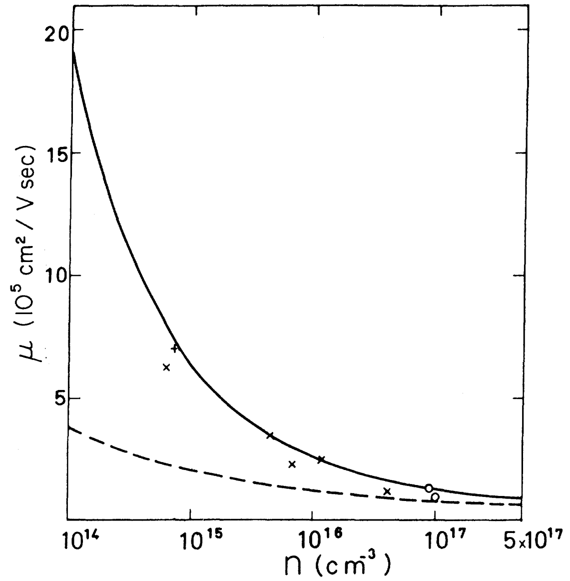


FIG. 2. Carrier mobility versus impurity concentration in $\alpha$-Sn. The solid line shows the calculated mobility with the enhanced dielectric constant. The dotted line is the calculated mobility with $\epsilon_0 = 24$. Experimental data at 4.2 °K are from Refs. 4 (plus signs), 7 (crosses), and 10 (open circles).

4.2 °K, the electron gas is degenerate at $10^{14}$ cm$^{-3}$ or above. At the upper limit $n = 5 \times 10^{17}$, the zero-gap screening is already negligible while at the same time the secondary valleys begin to be populated and the mobility has an abrupt change[12] due to a different mechanism discussed by Robinson and Rodriguez.[13] For comparison we also show on the same figure the calculated mobility value using a constant $\epsilon_0 = 24$. The agreement between the calculated curve using enhanced dielectric constant and the experimental values is excellent. On the other hand, without invoking the dielectric enhancement, Broerman[14] has also produced an excellent fit to the mobility data by simply using Bloch waves to evaluate the impurity scattering cross section. Therefore, the excellent agreement achieved by us may be somewhat coincidental.

## IV. DISCUSSION

We would like to discuss other zero-gap materials. Do they all possess an enhanced dielectric constant? We shall discuss this question in terms of the existence of dielectric singularity in a pure sample, since this singularity has the same origin as the dielectric enhancement in a doped sample. For this class of materials, the zero energy gap may be required by symmetry or may be accidental. The coupling matrix element $|M|^2$ in Eq.

(2.2) should have quite different behavior in the two cases. Note that $|M|$ is just the overlap integral between the spatially periodic part of the two Bloch functions. When the two bands touch each other accidentally, $|M|^2$ behaves like $q^2$ in the small-$q$ limit. On the other hand, if the degeneracy of the band edge is symmetry induced as in $\alpha$-Sn, the strong mixing between conduction and valence states should make $|M|^2$ a constant in the small-$q$ limit for initial and final states in the vicinity of the band edge ($k<q$) as can be seen from Eq. (2.3). When $|M|^2 \to$ const and the energy difference between conduction and valence states near the band edge ($k<q$) goes like $q^2$, the contribution of states in the region $k<q$ should give a dielectric constant which behaves like $\lambda/q$ as $q\to 0$ according to Eq. (2.2). This has been confirmed by detailed calculations.[1,2] But when $|M|^2\to q^2$, the dielectric constant behaves like $q$ as $q\to 0$ and the singularity does not exist. As a result, material with zero energy gap which is not required by symmetry has no concentrational-dependent dielectric constant. The value of this dielectric constant depends on the average energy gap just as in any ordinary semiconductor.

We note that the dielectric enhancement discussed here has not been found in optical experiments.[5] The absence of enhancement at optical frequency is expected from qualitative considerations. Detailed investigation of the frequency dependence of the dielectric constant for both pure and doped $\alpha$-Sn by Sherrington and Kohn[15] also confirms this point.

A condensed version of this paper has been published elsewhere.[16]


## ACKNOWLEDGMENTS

The authors would like to thank Professor K. Singwi and Professor A. W. Ewald for very helpful discussions. One of us (L. L.) thanks Professor F. Bassani for the hospitality extended him at the Institute of Physics, the University of Pisa.


## APPENDIX A: EVALUATION OF $\alpha^{\text{inter}}$

Taking the matrix element given in (2.3) and making the spherical-band approximation with $m_e^*/m_h^* \ll 1$, $\epsilon^{\text{inter}}(q)$ in (2.2) is given by

$$\epsilon^{\text{inter}}(q) = 1 + \frac{6e^2 m_e^*}{\pi\hbar^2 q}\int\int dx\,d\mu\,\frac{x^2(1-\mu^2)}{(1+2x\mu+x^2)^2}\ , \quad \text{(A1)}$$

where we have put $x=k/q$ and $\mu=\vec{k}\cdot\vec{q}/kq$ in (2.2) and turned the summation over $\vec{k}$ into an integration in $k$ space. Because of the spherical-band approximation, both the conduction- and valence-band states are contained in a sphere of radius $K$ in $k$ space. Concentric with the conduction sphere, we draw another sphere of radius $k_F$ containing

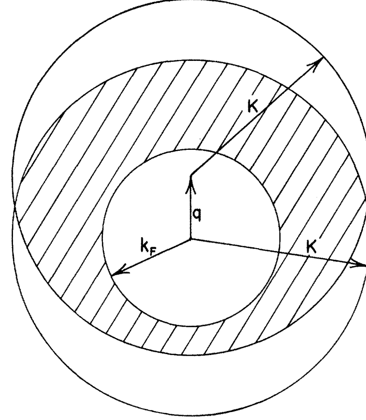


FIG. 3. Section through the centers of spheres showing the integration domain (shaded region) for the case $q<k_F<K-q$.

states occupied by the donor electrons. We displace the common center of these two spheres with respect to the center of the valence sphere by a distance $q$. The integration is performed in the overlap region between the valence sphere and the space bounded by the two concentric spherical surfaces. The origin for $x$ in (A1) is placed at the center of the valence sphere. We show the integration domain for the case $K-q>k_F>q$ by the shaded region in Fig. 3.

There appears a constant term in $\epsilon^{\text{inter}}(q)$ when the integral in (A1) is worked out. However its value is of no concern to us because we have already decided to rely upon experiments for the value of $\epsilon_0$. Ignoring a constant, we obtain the complete result for $4\pi\alpha^{\text{inter}}$ below:

$$4\pi\alpha^{\text{inter}}(q) = (6e^2 m_e^*/\pi\hbar^2 q)(I+I_l)\ . \quad \text{(A2)}$$

The function $I$ is given by

$$\begin{aligned} I = &-\frac{1}{16}-\frac{1}{8}\left(\frac{K}{q}+\frac{q}{K}\right)+\frac{3}{32}\left(\frac{q}{K}\right)^2 \\ &-\frac{1}{8}\frac{(K^2-q^2)^2}{k^2q^2}\ln\left(1-\frac{q}{K}\right)+\frac{1}{4}\left[\ln\left(1-\frac{q}{K}\right)\right]^2 \\ &-\frac{1}{2}\sum_{n=1}\frac{1}{n^2}\left(\frac{q}{K}\right)^n-\sum_{n=0}^{\infty}\frac{1}{(2n+1)^2}\left(\frac{q}{K-q}\right)^{2n+1} \\ &+\frac{1}{2}\sum_{n=1}^{\infty}\frac{1}{n^2}\left(\frac{q}{K-q}\right)^n-\frac{1}{4}\left(\frac{k_F}{q}-\frac{q}{k_F}\right) \\ &-\frac{1}{8}\left(\frac{q^2}{k_F^2}-\frac{k_F^2}{q^2}+4\ln\frac{k_F}{q}\right)\ln\frac{k_F+q}{|k_F-q|} \\ &+\frac{1}{4}\left[\ln\left(1+\frac{k_F}{q}\right)\right]^2+\frac{1}{2}\sum_{n=1}^{\infty}\frac{1}{n^2}\left(\frac{q}{k_F+q}\right)^n\ . \end{aligned} \quad \text{(A3)}$$

The subscript $l$ for $I_l (l = 1, 2, 3)$ is used to specify three different ranges of $q$ values. These three ranges together with the appropriate $I_l$ are given below:

*case* (1) $\frac{1}{2}k_F \geq q \geq 0$:

$$I_1 = -\frac{1}{4}\left[\ln\left(\frac{k_F}{q} - 1\right)\right]^2 + \sum_{n=0}^{\infty} \frac{1}{(2n+1)^2}\left(\frac{q}{k_F - q}\right)^{2n+1} - \frac{1}{2}\sum_{n=1}^{\infty} \frac{1}{n^2}\left(\frac{q}{k_F - q}\right)^n , \tag{A4}$$

*case* (2) $k_F \geq q \geq \frac{1}{2}k_F$:

$$I_2 = \frac{\pi^2}{12} + \frac{1}{2}\sum_{n=1}^{\infty} \frac{1}{n^2}\left(\frac{k_F}{q} - 1\right)^n - \sum_{n=0}^{\infty} \frac{1}{(2n+1)^2}\left(\frac{k_F}{q} - 1\right)^{2n+1} , \tag{A5}$$

*case* (3) $q \geq k_F$:

$$I_3 = \frac{\pi^2}{12} + \frac{1}{2}\sum_{n=1}^{\infty} \frac{1}{n^2}\left(1 - \frac{k_F}{q}\right)^n . \tag{A6}$$

We may put

$$f(q) = (k_F/q)(I + I_l) + O'(q) \tag{A7}$$

to express $4\pi\alpha^{\text{inter}}$ in terms of $f(q)$ as in (2.4), where $O'(q)$ is some function whose value is negligibly small for small $q$.

## APPENDIX B: VALIDITY OF BORN APPROXIMATION

In discussing the question of validity we neglect the $q$ dependence of $\epsilon_I$ and assume a Yukawa form for the screened impurity potential, i.e.,

$$V_s(r) \simeq -\frac{e^2}{\epsilon_I(0)} \frac{e^{-k_{\text{FT}}^{\text{eff}}(0)r}}{r} . \tag{B1}$$

In considering the scattering of electrons of effective mass $m_e^*$ and momentum $k_F$ by the potential in (B1), the condition for validity[17] of the Born approximation for $k_F > k_{\text{FT}}^{\text{eff}}$ ($k_F/k_{\text{FT}}^{\text{eff}} \sim 2$–$4$ for $n = 10^{12}$–$10^{18}$ cm$^{-3}$) becomes

$$[m_e^* e^2/\epsilon_I(0)\hbar^2 k_F] \ln[k_F/k_{\text{FT}}^{\text{eff}}(0)] \ll 1 . \tag{B2}$$

Expressing $k_{\text{FT}}^{\text{eff}}$ in terms of $k_F$, i.e.,

$$k_{\text{FT}}^{\text{eff}} = \{[1/\epsilon_I(0)][4m_e^* e^2/\pi\hbar^2]\, k_F\}^{1/2} , \tag{B3}$$

we can rewrite the validity condition in (B2) as

$$[2\epsilon_I(0)\alpha_\infty^* k_F]^{-1} \ln[\tfrac{1}{4}\pi\,\epsilon_I(0)\alpha_\infty^* k_F] \ll 1 , \quad \tfrac{1}{4}\pi\,\epsilon_I(0)\alpha_\infty^* k_F \gg 1, \tag{B4}$$

where $\alpha_\infty^*$ is the effective Bohr radius. It is seen that the condition in (B4) is satisfied as the factor $\epsilon_I(0)\alpha_\infty^* k_F$ is always greater than 1 for the values of impurity concentration under consideration.

## APPENDIX C: EVALUATION OF $A$

Using the ansatz (3.5), the screened impurity potential $V_s(q)$ becomes

$$V_s(q) = -V_s^{\text{Yukawa}}\left[1 - \left(1 - \frac{\epsilon_0}{\epsilon_I(0)}\right) a \frac{q^4}{[q^2 + k_{\text{FT}}^{\text{eff}}(0)^2]k_F^2}\right]^{-1} , \tag{C1}$$

where

$$V_s^{\text{Yukawa}} = 4\pi e^2/\epsilon_I(0)[q^2 + k_{\text{FT}}^{\text{eff}}(0)^2] .$$

By keeping terms only to first order in $a$, the differential cross section according to (3.6) can be expressed as the sum of two contributions:

$$\sigma(\theta) = \sigma_Y + \sigma_c , \tag{C2}$$

where $\sigma_Y = |(m_e^*/2\pi\hbar^2)V_s^{\text{Yukawa}}(q)|^2$ arises from the Yukawa potential, and $\sigma_c$ is given by

$$\sigma_c = \frac{8a}{[\epsilon_I(0)\alpha_\infty^* k_F]^2}\left(1 - \frac{\epsilon_0}{\epsilon_I(0)}\right) \frac{q^4}{[q^2 + k_{\text{FT}}^{\text{eff}}(0)^2]^3} . \tag{C3}$$

It is remarked here that the expansion in powers of $a$ is valid because the largest value for the second term inside the bracket in Eq. (C1) (at $q = 2k_F$) at impurity concentration as high as $10^{18}$ cm$^{-3}$ is about $\frac{1}{4}$. Therefore, we can neglect terms of order $a^2$ or higher since we are only aiming at 10% accuracy in our results.

Corresponding to $\sigma_Y$ and $\sigma_c$ in (C2), the total cross section for momentum transfer in (3.3) can be split into two terms:

$$A = A_Y + A_c . \tag{C4}$$

The Yukawa term $A_Y$ has been calculated[9] and we quote the results below:

$$A_Y = \frac{2\pi g(b)}{k_F^2[\epsilon_I(0)\alpha_\infty^* k_F]^2} , \tag{C5}$$

where

$$g(b) = \ln(1 + b) - b/(1 + b) , \tag{C6}$$

$$b = \pi\epsilon_I(0)\alpha_\infty^* k_F . \tag{C7}$$

The term $A_c$ is equal to the following integral:

$$A_c = \frac{8\pi a}{k_F^2[\epsilon_I(0)\alpha_\infty^* k_F]^2}\left(1 - \frac{\epsilon_0}{\epsilon_I(0)}\right) \times \oint d\theta \frac{\sin^6(\frac{1}{2}\theta)\sin\theta}{\{\sin^2(\frac{1}{2}\theta) + [k_{\text{FT}}^{\text{eff}}(0)/2k_F]^2\}^3} . \tag{C8}$$

The integral is evaluated to be just 2 by neglecting the term $k_{FT}^{eff}/2k_F$ in the denominator of the integrand. We obtain then

$$A_c = \frac{16\pi a[1 - \epsilon_0/\epsilon_I(0)]}{k_F^2[\epsilon_I(0)a_\infty^* k_F]^2} \quad . \tag{C9}$$

*Supported in part by National Science Foundation Grant No. GP7703 and Advanced Research Projects Agency (through Northwestern University Materials Research Center).


[1]L. Liu and D. Brust, Phys. Rev. Letters 20, 651 (1968); Phys. Rev. 173, 777 (1968).

[2]D. Sherrington and W. Kohn, Rev. Mod. Phys. 40, 767 (1968); B. I. Halperin and T. M. Rice, *ibid.* 40, 755 (1968).

[3]S. H. Groves and W. Paul, Phys. Rev. Letters 11, 194 (1963).

[4]C. F. Lavine and A. W. Ewald (unpublished); C. F. Lavine, thesis, Northwestern University (unpublished).

[5]R. E. Lindquist and A. W. Ewald, Phys. Rev. 135, A191 (1964).

[6]P. Nozieres and D. Pines, Nuovo Cimento 9, 470 (1958); Phys. Rev. 109, 762 (1958); H. Ehrenreich and M. H. Cohen, *ibid.* 115, 786 (1959).

[7]E. D. Hinkley and A. W. Ewald, Phys. Rev. 134, A1261 (1964).

[8]R. J. Wagner and A. W. Ewald, Bull. Am. Phys. Soc. 11, 829 (1966); R. J. Wagner, thesis, Northwestern University, 1967 (unpublished).

[9]R. B. Dingle, Phil. Mag. 46, 831 (1955).

[10]O. N. Tufte and A. W. Ewald, Phys. Rev. 122, 1431 (1961).

[11]L. Liu and D. Brust, Phys. Rev. 157, 627 (1967).

[12]B. L. Booth and A. W. Ewald, Phys. Rev. Letters 18, 491 (1967).

[13]J. E. Robinson and S. Rodriguez, Phys. Rev. 135, A779 (1964); 137, A663 (1965).

[14]J. G. Broerman, Phys. Rev. Letters 24, 450 (1970).

[15]D. Sherrington and W. Kohn, Phys. Rev. Letters 21, 153 (1968).

[16]L. Liu and E. Tosatti, Phys. Rev. Letters 23, 772 (1969).

[17]L. I. Schiff, *Quantum Mechanics* (McGraw-Hill, New York, 1960), p. 169.


PHYSICAL REVIEW B VOLUME 2, NUMBER 6 15 SEPTEMBER 1970

# Brillouin Scattering Study of Propagating Acoustoelectric Domains in *n* GaAs†*

David L. Spears‡

*Department of Physics, Purdue University, Lafayette, Indiana* 47907

(Received 15 September 1969)

A Brillouin-scattering study of amplified shear waves in propagating acoustoelectric domains in *n* GaAs is presented. On the basis of small-signal theory, a complete formalism is developed for the amplification of piezoelectrically active waves from the thermal background of lattice vibrations. Our experimental results show that this provides a good description of the acoustic flux when its intensity is less than about $10^{-2}$ J/cm$^3$. Here, the growth rate, intensity, frequency distribution, angular distribution, and spatial distribution of the amplified shear waves were all found consistent with small-signal theory. In the subsequent stages of growth, when the acoustic waves become very intense, many interesting deviations from small-signal theory were found, resulting from at least two nonlinear effects, parametric frequency conversion, and enhanced electron-phonon coupling. The acoustic spectrum is rapidly extended to low frequencies, with relatively narrow domains being initially produced at these frequencies. The acoustic energy density tends to saturate at about 1 J/cm$^3$.

## I. INTRODUCTION

It is well known that injected ultrasonic waves can be amplified in piezoelectric semiconductors by the application of a sufficiently high electric field[1] because of the strong interaction with mobile charge carriers.[2] When the drift velocity exceeds the sound velocity, energy and momentum are transferred from the carriers to the acoustic wave.[3] Such interaction with internally generated acoustic waves has been used to explain the electrical instabilities observed in many piezoelectric semiconductors (CdS,[4] GaAs,[4] CdSe,[5] ZnO,[6] Te,[7] ZnS,[8] GaSb,[9] and InSb[10]). These instabilities generally show up as either damped or continuous oscillations in the current. The continuous oscillations are characterized by a high-field domain which propagates with the velocity of sound in the